International Immunopharmacology 75 (2019) 105758

Contents lists available at ScienceDirect

International Immunopharmacology

journal homepage: www.elsevier.com/locate/intimp

Bortezomib ameliorates acute allograft rejection after renal transplant by inhibiting Tfh cell proliferation and differentiation *via* miR-15b/IRF4 axis

Lei Liu[1], Zhi-gang Wang[1], Xin-lu Pang, Yong-hua Feng, Jun-xiang Wang, Hong-chang Xie, Xian-lei Yang, Jin-feng Li[*], Gui-wen Feng[*]

Department of Kidney Transplantation, The First Affiliated Hospital of Zhengzhou University, Zhengzhou 450000, Henan Province, China

ARTICLE INFO

Keywords:
Bortezomib
Allograft rejection
T follicular helper cells
Proliferation
Differentiation
miR-15b
IRF4

ABSTRACT

Objective: The present study aimed to investigate the functional role of bortezomib in the development of acute allograft rejection (AR) after renal transplant.

Methods: The mouse model of AR was established by allograft kidney transplant followed by the treatment of bortezomib. The serum cytokines, renal function, and the percentage of T follicular helper (Tfh) cells in $CD4^+$ T cells were measured. The effect of miR-15b and interferon-regulatory factor 4 (IRF4) on Tfh cell proliferation and differentiation was assessed by cell transfection technology and CCK-8 assay. The interaction between miR-15b and IRF4 was assessed by luciferase reporter assay.

Results: Bortezomib relieved acute AR after renal transplant by suppressing Tfh cell proliferation and differentiation. Meanwhile, bortezomib treatment markedly increased miR-15b expression in AR renal tissues. The upregulation of miR-15b inhibited Tfh cell proliferation and differentiation by reducing IRF4. In addition, bortezomib ameliorated AR by suppressing Tfh cell proliferation and differentiation through miR-15b/IRF4 axis *in vitro* and *in vivo*.

Conclusion: Our findings indicated the mechanism underlying the bortezomib in treating acute AR after renal transplant, and suggested the critical role of miR-15b in Tfh cell proliferation and differentiation, which provided a therapeutic target in attenuating acute AR.

1. Introduction

Renal transplant is considered as the ideal therapy for patients with end-stage renal disease (ESRD) such as renal failure, and it has been proven to dramatically improve the prognosis and early survival rate of these patients [1]. However, postoperative allograft rejection (AR) remains a risk factor for the long-term graft survival [2]. It is well known that the AR after renal transplant consists of several steps including antigen recognition, lymphocyte proliferation and differentiation, and target cells injury, leading to a series of immunoreactions [3]. Therefore, it is crucial to identify the mechanism behind AR in order to find out the preventive and therapeutic strategies of AR.

Several studies have suggested that the incidence of AR was observably decreased with the use of novel immunosuppressive agents, such as actinomycin D [4] and alemtuzumab [5]. As a highly selective proteasome inhibitor approved by the Food and Drug Administration (FDA), bortezomib has been initially used for the treatment of multiple myeloma by specifically eliminating activated plasma cells [6]. It has been proven that bortezomib had a stronger humoral immunosuppressive effects relative to conventional drugs, such as rituximab [7], and recent studies have demonstrated the therapeutic effect of bortezomib on AR after renal transplant [8–10]. Evidence has showed that bortezomib may stabilize estimated glomerular filtration rate (eGFR) for 3–6 months in pediatric kidney transplant recipients with antibody-mediated rejection [8]. Nevertheless, little is known concerning the action mechanism of bortezomib in acute AR after kidney transplant.

The IFN-regulatory factor (IRF) family were originally identified as transcriptional regulators in the type I interferon system, consisting of nine members in mammals. Indeed, it has recently been shown that IRF family performed versatile functions in various biological processes containing immunoreaction, cytokine signal transduction as well as cell proliferation and regulatory mechanism [11]. Remarkably, IRFs played crucial roles in regulating T-helper (Th) cell differentiation.

[*] Corresponding authors at: Department of Kidney Transplantation, The First Affiliated Hospital of Zhengzhou University, 1 Jianshe Rd., Erqi District, Zhengzhou 450000, Henan Province, China.
E-mail address: queping311137@163.com (G.-w. Feng).
[1] Lei Liu and Zhi-gang Wang are co-first authors.

https://doi.org/10.1016/j.intimp.2019.105758
Received 16 May 2019; Received in revised form 10 July 2019; Accepted 10 July 2019
Available online 01 August 2019

Particularly, IRF1 was decisive for Th1 cell generation while IRF4 controlled Th2, Th9 and Th17 cell differentiation [12]. Previous studies have demonstrated that IRF4 was also an intrinsic prerequisite for B cell differentiation and plasma cell maturation, devoting itself to positively regulating Tfh cell differentiation [13].

MicroRNAs (miRNAs), noncoding small RNAs containing endogenous 21–23 nucleotides, were involved in regulating eukaryotic gene expression post-transcriptionally *via* binding to 3′-UTR of mRNA of the target genes. Increasing miRNAs dysregulation has been noted in circulating immune after renal transplant [14], implying their potential roles in the renal insufficiency. For instance, Matz et al. [15] found that miR-15b expression was significantly decreased in patients with T-cell mediated rejection together with urinary tract infection as opposed to patients with stable graft function. Moreover, Singh et al. [16] reported that miR-15b overexpression in $CD4^+$ T cells promoted the induction of regulatory T cells (Tregs), downregulating the autoimmune response. A recent study reported that bortezomib treatment induced an upregulation of miR-15b expression in hepatocellular carcinoma cells [17]. Thus, the present study aimed to discover the underlying molecular mechanisms and biological function of bortezomib in AR after kidney transplant.

2. Material and methods

2.1. AR model and animal grouping

12–14 weeks of male C57BL/6 mice ($H2^b$) and female BALB/c mice ($H2^d$) weighing 24–28 g obtained from Center for Animal Experiment of Henan province (Zhengzhou, Henan, China) were used as donors and recipients, respectively, in this study. The mouse model of renal transplant was established as previously described [18], mice with acute AR after renal transplant were enrolled, while mice with early complications including thrombus, bleeding, and urinary fistule were excluded and immediately sacrificed. In brief, mice underwent a standard midline abdominal incision under anesthesia with inhalation of 2% isoflurane (Abbott GmbH, Vienna, Austria). Then, the left kidneys of donors along with aorta, inferior vena cava and ureter were removed under a microscope followed by lavage *in situ* with histidine-tryptophane-ketoglutarate (HTK) solution. The isolated kidneys were then implanted below the level of native renal vessels of recipients with left nephrectomy, while the infrarenal aorta and the inferior vena cava were perfectly anastomosed to the recipients. In addition, the ureter was directly anastomosed into the bladder for urinary tract reconstruction. Mice were randomized into 4 groups (n = 7 in each group): auto kidney transplant group (auto TX), stable graft function without AR (Stable), AR group, and bortezomib treatment group. Auto kidney transplant was performed in the BALB/c mice. In the bortezomib treatment group, bortezomib (LC Laboratories, Woburn, MA, USA) that was dissolved in dimethyl sulfoxide (DMSO) and then diluted in 100 mL sterile normal saline was intravenously administered to the recipients at a dose of 1.3 mg/m^2 on the day 1, 4, 8, and 11 following the surgery. After 2 weeks, the serum creatinine and mean eGFR were detected, and then the mice were euthanatized and blood samples were collected for measuring serum levels of IFN-γ, TNF-α, IL-2, IL-4, and IL-10. Kidney tissues were dissected for HE staining, immunohistochemistry staining, and for detection of the percentage of Tfh cells ($CD4^+$ $CXCR5^+$). All animal protocols were approved by the Institutional Animal Care and Use Committee at the First Affiliated Hospital of Zhengzhou University and performed compliance with the Guide for the Care and Use of Laboratory Animals.

2.2. Serum levels of cytokines

The serum levels of regulatory and pro-inflammatory cytokines including IFN-γ, TNF-α, IL-2, IL-4 and IL-10 were assessed as biomarkers of allograft function using the enzyme-linked immunosorbent assay (ELISA) kit (R&D Systems, Minneapolis, MN, USA) following the manufacturer's instructions. Each blood sample was tested in duplicate.

2.3. Assessment of renal function

Renal function was assessed with the serum creatinine utilizing SOE assay (Shanghai Kehua Dongling Diagnostic Products, Shanghai, China) and eGFR calculated by the abbreviated MDRD equation based on serum creatinine measurements. In short, blood samples were centrifuged at 3600 rpm for 10 min. The absorbance at wavelength of 546 nm was measured after supernatant was incubated in mixed solution containing creatine hydrolyzyme, sarcosine oxidase and catalase at 37 °C for 5 min.

2.4. Cell isolation and cell transfection

Tfh cells separated from inguinal lymph nodes of mice in AR group were enriched by magnetic activated cell sorting (MACS), sorted using CXCR5 as well as Programmed Death 1 (PD-1) as additional markers on an ARIA II flow sorter (BD Biosciences, San Diego, CA, USA). Tfh cells were transfected with miR-15b mimic or pre-NC (negative control of miR-15b mimic) (Shanghai GenePharma Co., Ltd., Shanghai, China) using Lipofectamine 2000 reagent (Invitrogen, Carlsbad, CA, USA) following the manufacturer's instructions. After 48 h of transfection, cells were collected for assessing cell proliferative capacity using CCK-8 assay.

$CD4^+$ T cells were isolated from peripheral blood mononuclear cells (PBMCs) derived from peripheral blood of mice in AR group by density gradient centrifugation using the EasySep™ Naïve $CD4^+$ T Cell Isolation Kit (Miltenyi Biotec, Gladbach, Germany). Subsequently, cells were seeded in 96-well plates at a density of 7.5×10^4 cells/well in AIM-V medium (Life Technologies, Carlsbad, CA, USA) supplemented with Dynabeads Human T-Activator CD3/CD28 (2 μl/well, Life Technologies), recombinant rat activin A (50 ng/ml, BD Biosciences) and recombinant human IL-12 (5 ng/ml, Peprotech, Rocky Hill, NJ, USA). After incubated at 37 °C with 5% CO_2 for consecutive 5 days, $CD4^+$ T cells were finally transfected with miR-15b mimic or pre-negative control. After 48 h, cells were harvested for detection of the proportion of Tfh cells using flow cytometry.

2.5. Luciferase reporter assay

The 3′-UTR fragments of IRF4 and the potential target sequences of miR-15b predicted by bioinformatics tools including Targetscan (http://www.targetscan.org) and microrna.org (http://www.microrna.org) were amplified and sub-cloned into pGL3 plasmids (Promega, Madison, WI, USA). HEK293T cells (American Type Culture Collection, Manassas, VA, USA) grown to about 70% confidence were seeded in 24-well plates and then co-transfected with 50 ng of pGL3-IRF-WT vectors or pGL3-IRF-MUT vectors along with miR-15b mimic/inhibitor or their corresponding empty vectors (pre-negative control/negative control) using Lipofectamine 2000 (Invitrogen). Luciferase activity was measured 24 h after transfection using a Dual-Luciferase Reporter 1000 Assay System (Promega) according to the manufacturer's instructions. In addition, the expression of IRF4 at mRNA and protein levels was measured using qRT-PCR and western blot after HEK293T cells were transfected with miR-15b mimic or inhibitor as well as pre-negative control or negative control (negative control of miR-15b inhibitor). Each experiment was conducted in triplicate. In this study, both the miRNA-15b mimic and inhibitor were synthesized by Shanghai GenePharma.

2.6. In vivo experiments

We also explored the function of bortezomib *in vivo*. AR mice were assigned into 3 groups (n = 7 in per group): control group, bortezomib

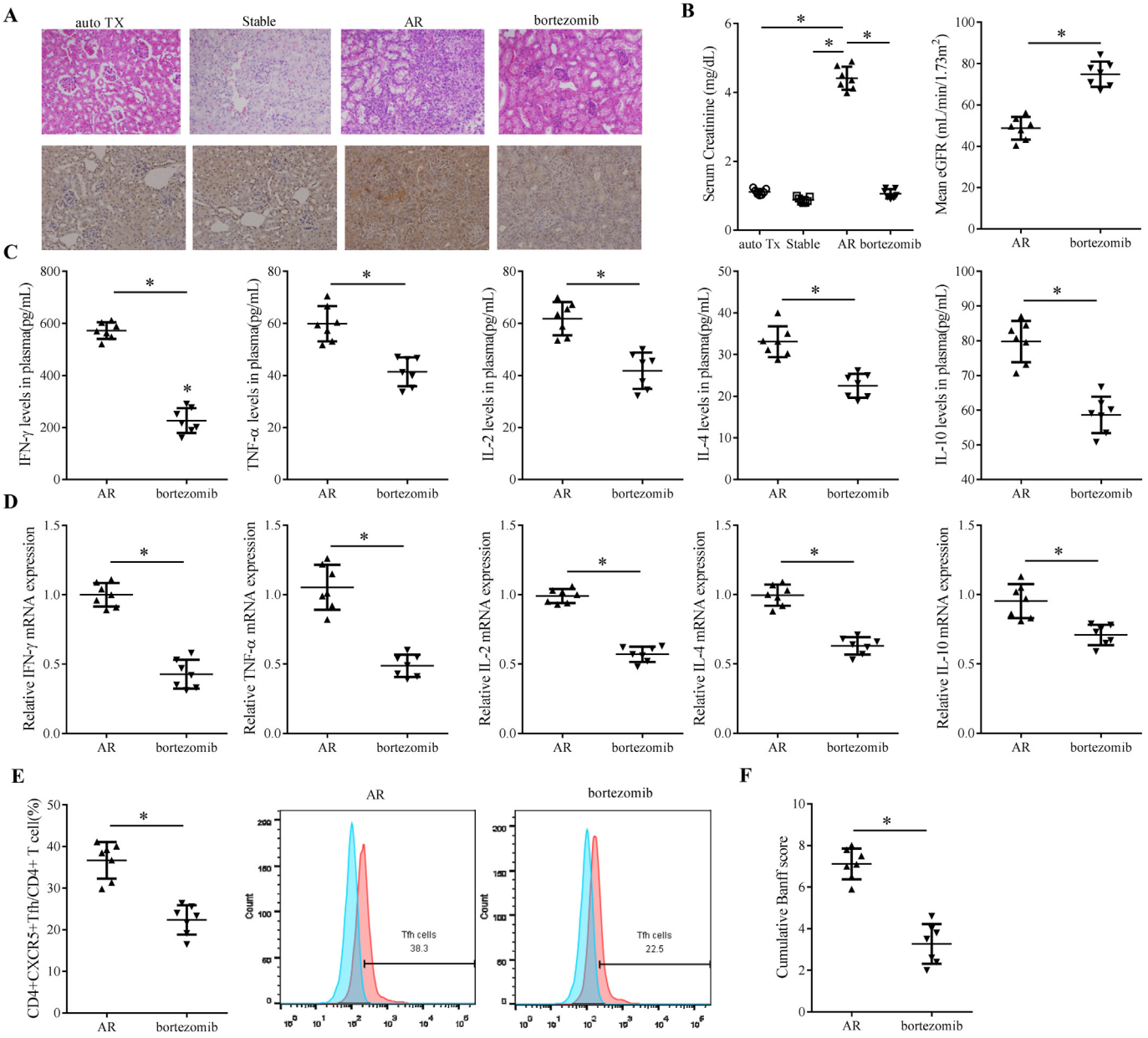

Fig. 1. The effect of bortezomib on acute rejection in a mouse model of renal allograft. The mouse model of AR was established by allograft kidney transplant followed by the treatment of bortezomib. Mice were randomized into 4 groups (n = 7 in each group): auto kidney transplant group (auto TX), stable graft function without AR (Stable), AR group, and bortezomib group. (A) HE staining and immunohistochemistry staining images of renal tissues; (B) serum creatinine and mean eGFR; (C) serum levels of IFN-γ, TNF-α, IL-2, IL-4, and IL-10 were detected using ELISA; (D) mRNA expression of the inflammatory cytokines in renal tissues was detected using qRT-PCR; (E) percentage of Tfh cells ($CD4^+$ $CXCR5^+$) in $CD4^+$ T cells in mouse renal tissues was detected using flow cytometry analysis; (F) Cumulative Banff score. *$P < 0.05$ compared with the AR group.

+negative control, and bortezomib + miR-15b inhibitor. Mice in bortezomib + negative control and bortezomib + miR-15b inhibitor group were intravenously injected with 1.3 mg/m^2 of bortezomib containing antagomir control or antagomir-15b (60 mg/kg body weight) *via* tail vein. 2 weeks later, with the serum creatinine and mean eGFR evaluated, all mice were sacrificed and the blood samples were taken for measuring serum levels of cytokines as well as the expression levels of miR-15b and IRF4. Flow cytometer was used to test the proportion of Tfh cells in kidney tissues.

2.7. Cell proliferation assay

After 48 h of transfection, Tfh cells were seeded into 96-well plates at a density of 2×10^3cells/well and cultured for 48 h. Cell proliferation was determined using cell counting kit-8 (CCK-8) assay (Beyotime) according to the manufacturer's protocol. Absorbance was detected at the wavelength of 450 nm.

2.8. Flow cytometry analysis

The kidney tissues were cut into pieces of approximately 2 mm^2, and digested by tyrosinase plus 0.5% type II collagenase (Gibco, Carlsbad, CA, USA) at 37 °C with 5% CO_2 for 1–2 h and meshed through a 200-gauge stainless steel filter. Cells were collected by centrifugation at 1500 rpm for 10 min at 4 °C and resuspended in PBS after supernatant was discarded. Single nucleus cell suspension was harvested for flow cytometry analysis.

The percentage of Tfh cells in the mouse kidney and activated naïve

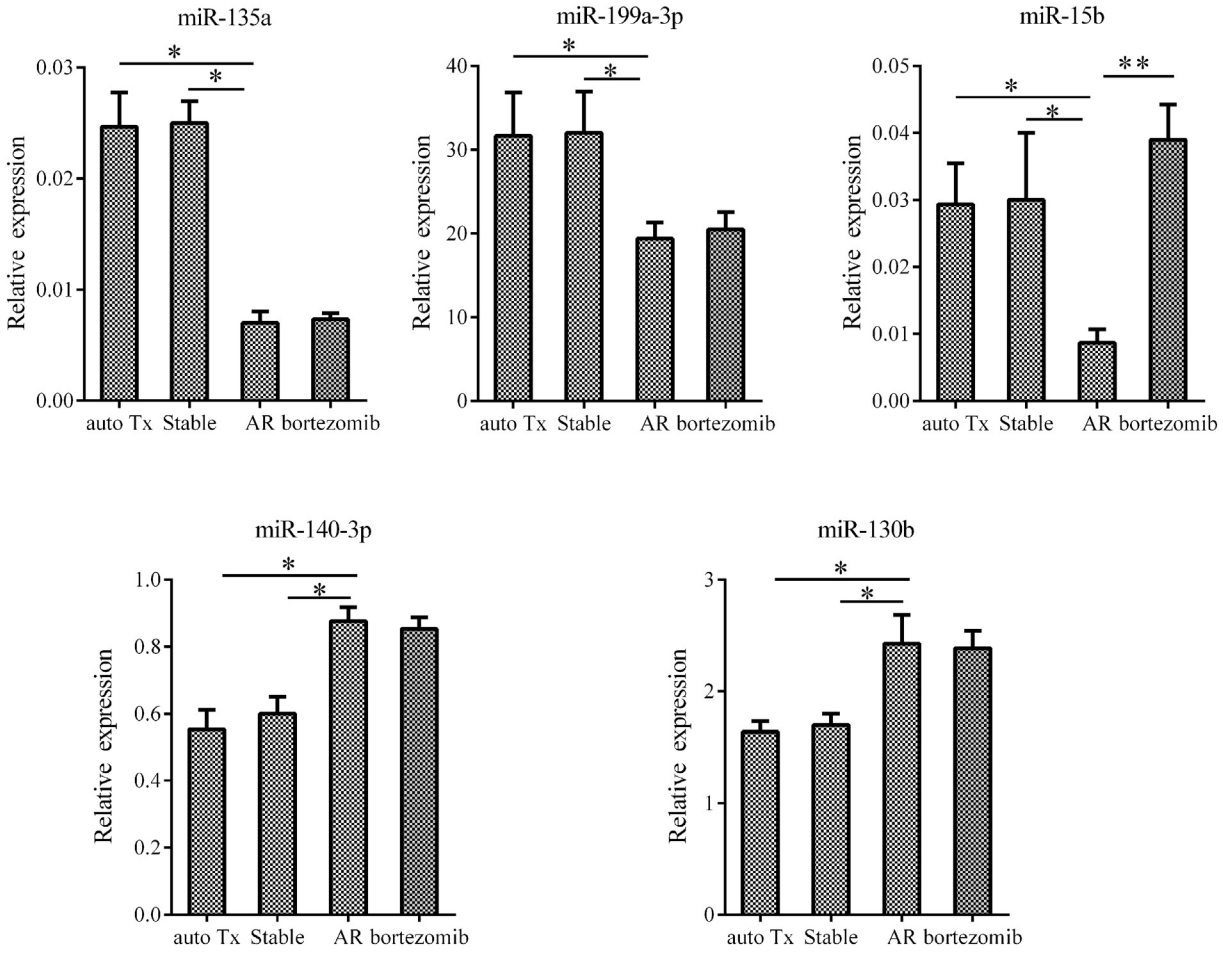

Fig. 2. The effect of bortezomib on miRNA expressions. The relative expression levels of miR-135a, miR-199a-3p, miR-15b, miR-140-3p and miR-130b in renal tissues of mice in auto TX, Stable, AR, and bortezomib groups (n = 7 in each group) were determined by qRT-PCR. *P < 0.05 compared with the auto TX or Stable group; **P < 0.05 compared with the AR group.

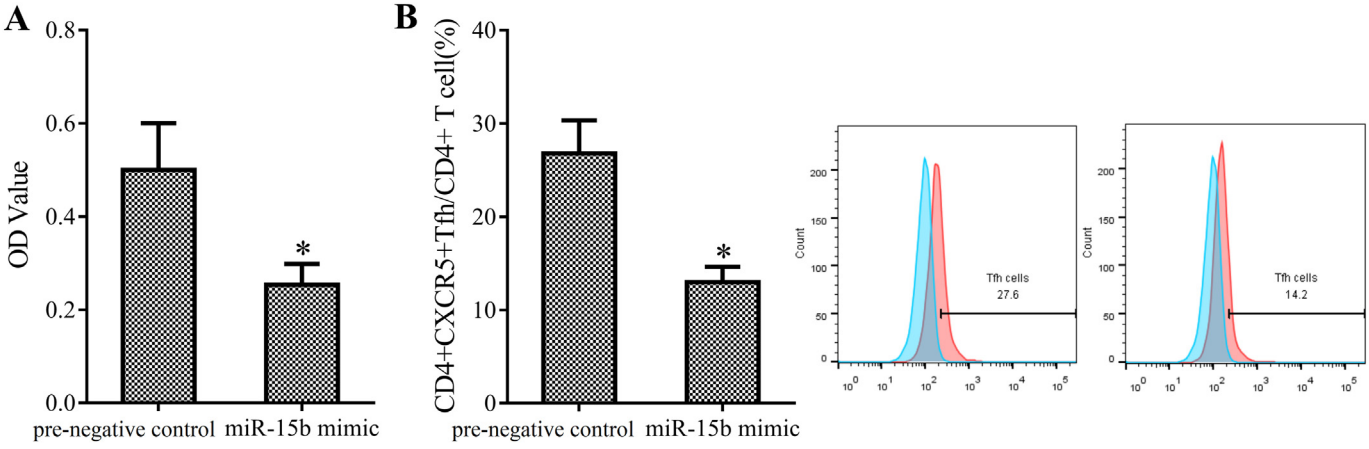

Fig. 3. The effect of miR-15b on the proliferation and differentiation of Tfh cells. Tfh cells were derived from lymph nodes of AR mice. $CD4^+$ T cells were isolated from peripheral blood of AR mice. Tfh and $CD4^+$ T cells were transfected with miR-15b mimic or pre-negative control. (A) Tfh cell proliferation was measured by CCK-8 assay; (B) proportion of Tfh cells ($CD4^+$ $CXCR5^+$) in $CD4^+$ T cells was analyzed using flow cytometry. *P < 0.05 compared with pre-negative control group.

$CD4^+$ T cells that isolated from PBMCs was also determined by flow cytometry. Briefly, cell suspension at 10^6/tube was stained in duplicate with FITC-anti-CD4 (eBioscience, San Diego, CA, USA) and PE-anti-CXCR5 (R&D Systems) at room temperature for 30 min in the dark. After being washed with PBS, the cells were subjected to flow cytometry detection on the FACSCalibur (BD Biosciences) with FACSDiva software (Tree Star, Ashland, OR, USA). At least 50,000 lymphocytes per sample were analyzed.

2.9. QRT-PCR

To detect relative expression levels of miR-135a, miR-199a-3p, miR-15b, miR-140-3p and miR-130b together with IRF4 mRNA, total RNA was extracted from the whole kidney tissues using Trizol reagent

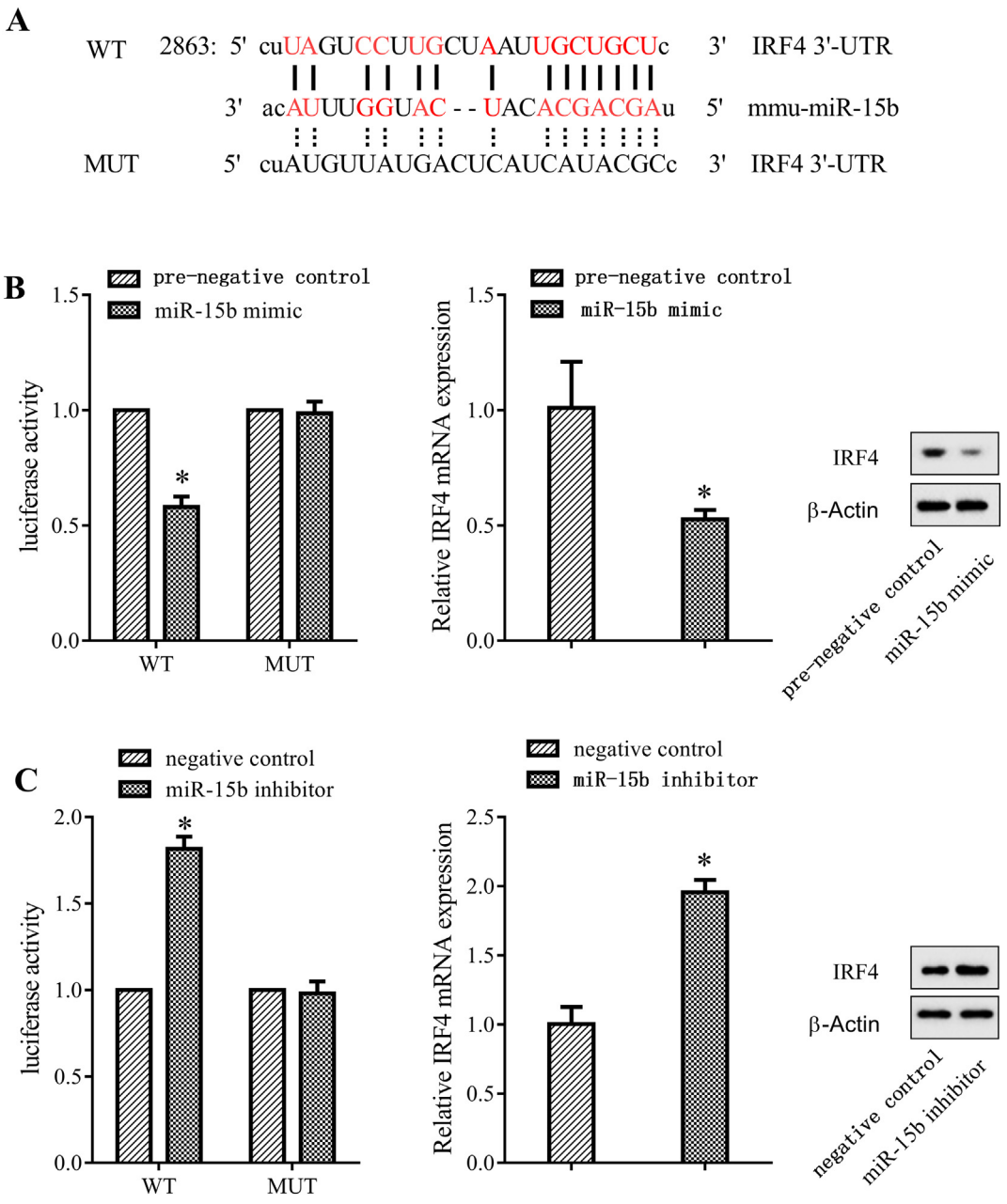

Fig. 4. The interaction between MiR-15b and IRF4. (A) Potential binding sites of miR-15b and IRF4 were predicted using bioinformatical analysis; (B) HEK293T cells were transfected with wild type (WT) or mutant (MUT) IRF4 3′-UTR luciferase reporter vectors and miR-15b mimic. The relative luciferase activity, the mRNA and protein expressions of IRF4 were determined; (C) HEK293T cells were transfected with WT or MUT IRF4 3′-UTR luciferase reporter vectors and miR-15b inhibitor. The relative luciferase activity, the mRNA and protein expressions of IRF4 were determined. $^{*}P < 0.05$ compared with the pre-negative control group; $^{\#}P < 0.05$ compared with the negative control group.

(Invitrogen) following the manufacturer's protocol. Total RNA was then reversely transcribed into cDNA using a MiRcute miRNA First-strand cDNA synthesis kit (Tiangen Biotech, Beijing, China) for miRNA or using Primer-Script TM one step RT-PCR kit (Takara, Shiga, Japan) for the reverse transcription of mRNAs. The SYBR Green I real time PCR kit (CoWin Bioscience Co., Beijing, China) was used to amplify targets on an ABI 7500 Real-Time PCR system (Applied Biosystems, Carlsbad, CA, USA) and calculated by the $2^{-\Delta\Delta Ct}$ method. The relative expression of mRNAs and miRNAs were normalized to β-action and U6 snRNA expression, respectively.

2.10. Western blot

Prior to western blotting, blood samples were diluted with saline solution, resuspended in lymphocyte separation medium and centrifuged at 3000 rpm for 25 min at 4 °C. Supernatant was removed and the remaining mononuclear cells were collected. The separated cells along with Tfh cells were washed once with cold PBS, incubated with Radio-Immunoprecipitation Assay (RIPA) buffer (Beyotime, Shanghai, China) for 30 min and centrifuged at 14,000 rpm for 15 min at 4 °C. Then, the cell extract was run on 10% SDS polyacrylamide gel electrophoresis (SDS-PAGE), transferred onto polyvinylidene fluoride (PVDF) membranes and blocked in 5% skim milk in tris buffered saline tween (TBST) at 4 °C overnight. Blots were probed with rabbit anti-mouse IRF-4 polyclonal antibody (1:250; Santa Cruz Biotechnology, Santa Cruz, CA, USA), then incubated with horseradish-peroxidase-coupled goat anti-rabbit antibodies (1:200; Abcam) at 37 °C for 2 h and visualized on a Molecular Imager ChemiDoc XRS System (Bio-Rad

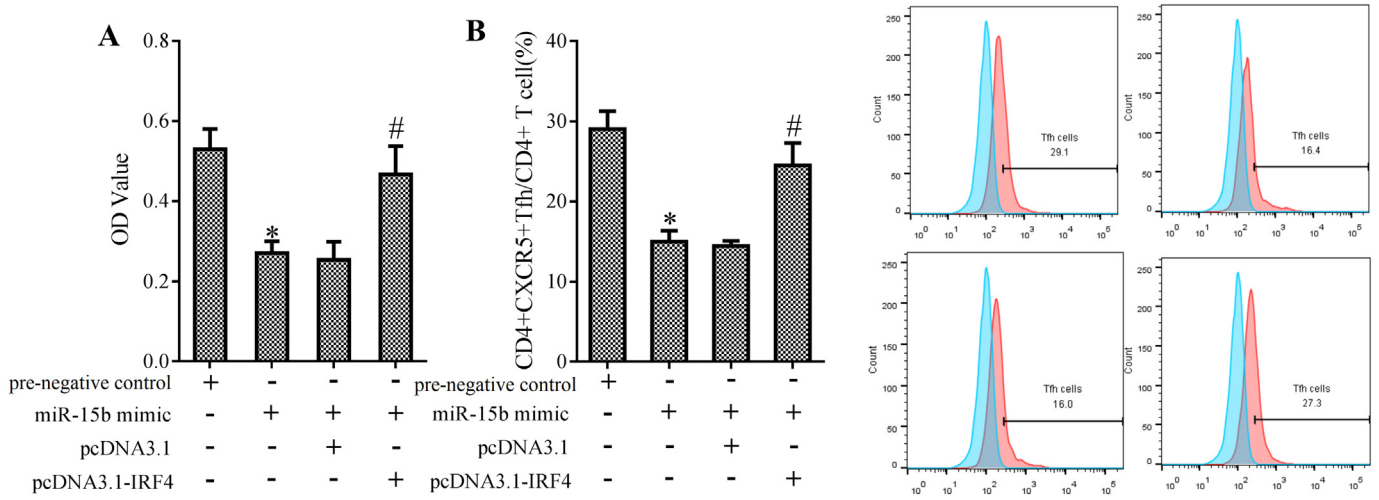

Fig. 5. miR-15b regulated Tfh cell proliferation and differentiation by targeting IRF4. Tfh cells were transfected with vectors and grouped into: pre-negative control, miR-15b mimic, miR-15b mimic + pcDNA3.1, and miR-15b mimic + pcDNA3.1-IRF4. (A) Tfh cell proliferation was measured by CCK-8 assay; (B) the percentage of Tfh cells ($CD4^+$ $CXCR5^+$) in $CD4^+$ T cells was analyzed using flow cytometry. *P < 0.05 compared with the pre-negative control group; #P < 0.05 compared with miR-15b mimic + pcDNA3.1 group.

Laboratories, Hercules, CA, USA) using an ECL Plus Western Blotting Substrate (Thermo Scientific, Shanghai, China). In addition, β-action (Sigma-Aldrich) served as an internal control.

2.11. Statistical analysis

Data were expressed as the mean ± standard deviation (S.D.). Comparisons between two groups were assessed by two-sided Student's *t*-test using the SPSS 22.0 (IBM, Armonk, NY, USA). The comparisons among groups were done using one-way analysis of variance (ANOVA), followed by Tukey *post hoc* testing. P < 0.05 was considered statistically significant.

3. Results

3.1. Bortezomib suppressed acute rejection in a mouse model of renal allograft

After renal transplant, about 10% mice in each group were discarded because of complications after kidney transplant. For the rest mice, the renal tissues were isolated for HE staining and immunohistochemistry staining to analyze the pathology of renal. As shown in Fig. 1A, much inflammatory cell infiltration was found in the AR group (n = 7) when compared with the auto TX (n = 7) and Stable group (n = 7), while it was relieved after bortezomib treatment (bortezomib, n = 7). Meanwhile, the serum creatinine was markedly higher in the AR group than in the auto TX and Stable group, but it was reduced in the bortezomib-treated group; and the mean eGFR was higher in the bortezomib-treated group than in the AR group (Fig. 1B, P < 0.05). The serum levels of typical pro-inflammatory cytokines including IFN-γ, TNF-α, IL-2, IL-4, and IL-10 were significantly decreased after bortezomib administration in a mouse AR model after renal transplant, in contrast to those in AR group (Fig. 1C, P < 0.05), as well as the mRNA expression of these inflammatory mediators (Fig. 1D, P < 0.05). Bortezomib treatment also resulted in the increased proportion of Tfh cells ($CD4^+$ $CXCR5^+$) in mouse kidney tissues (Fig. 1E, P < 0.05), which indicated the increase of Tfh cells differentiation. Cumulative Banff score was notably lower in the bortezomib-treated mice than that in the AR group (Fig. 1F, P < 0.05). All these data demonstrated that bortezomib ameliorated acute AR in mouse after renal transplant.

3.2. Bortezomib significantly upregulated miR-15b in AR

To identify which miRNA changed in response to bortezomib administration in acute AR after renal transplant, the expression levels of several representative miRNAs, which were reported to participate in the acute rejection after kidney transplant [19], were evaluated in the whole kidney tissues of the mice in the four groups (auto TX, Stable, AR, bortezomib; n = 7 in each group). The results showed that the expression levels of miR-135a, miR-199a-3p and miR-15b were lower while miR-140-3p and miR-130b were higher in AR group relative to the auto TX and Stable group (Fig. 2, P < 0.05). However, only miR-15b was observably upregulated after bortezomib treatment (bortezomib group) as compared with the AR group, while no significant difference was found in the expression of miR-135a, miR-199a-3p, miR-140-3p, and miR-130b (Fig. 2, P < 0.05). These findings illustrated that bortezomib led to a clear upregulation of miR-15b expression in a mouse model of acute renal AR, which may be associated with its effect on suppressing acute allograft rejection.

3.3. MiR-15b overexpression inhibited the proliferation and differentiation of Tfh cells

To further study the role of miR-15b in regulating the proliferation and differentiation of Tfh cells, the Tfh cells derived from lymph gland and $CD4^+$ T cells were transfected with miR-15b mimic or pre-negative control. It was shown that the growth of Tfh cells was inhibited after miR-15b mimic transfection (Fig. 3A, P < 0.05). As expected, miR-15b overexpression descended the percentage of Tfh cells in $CD4^+$ T cells (Fig. 3B, P < 0.05). Taken together, miR-15b overexpression exerted inhibitory effect on the proliferation and differentiation of Tfh cells.

3.4. MiR-15b negatively regulated IRF4

Bioinformatics analysis used for predicting recognition sequences on IRF4 revealed the presence of miR-15b binding sites (Fig. 4A). We further examined whether IRF4 was a direct target gene of miR-15b by using luciferase reporter assay. Our data manifested that in IRF4-WT group, miR-15b mimic induced a prominently reduction of luciferase activity in comparison with the pre-negative control group (Fig. 4B, P < 0.05), whereas, miR-15b inhibitor led to an enhanced luciferase activity relative to the negative control group (Fig. 4C, P < 0.05). In contrast, neither miR-15b mimic nor inhibitor notably affected

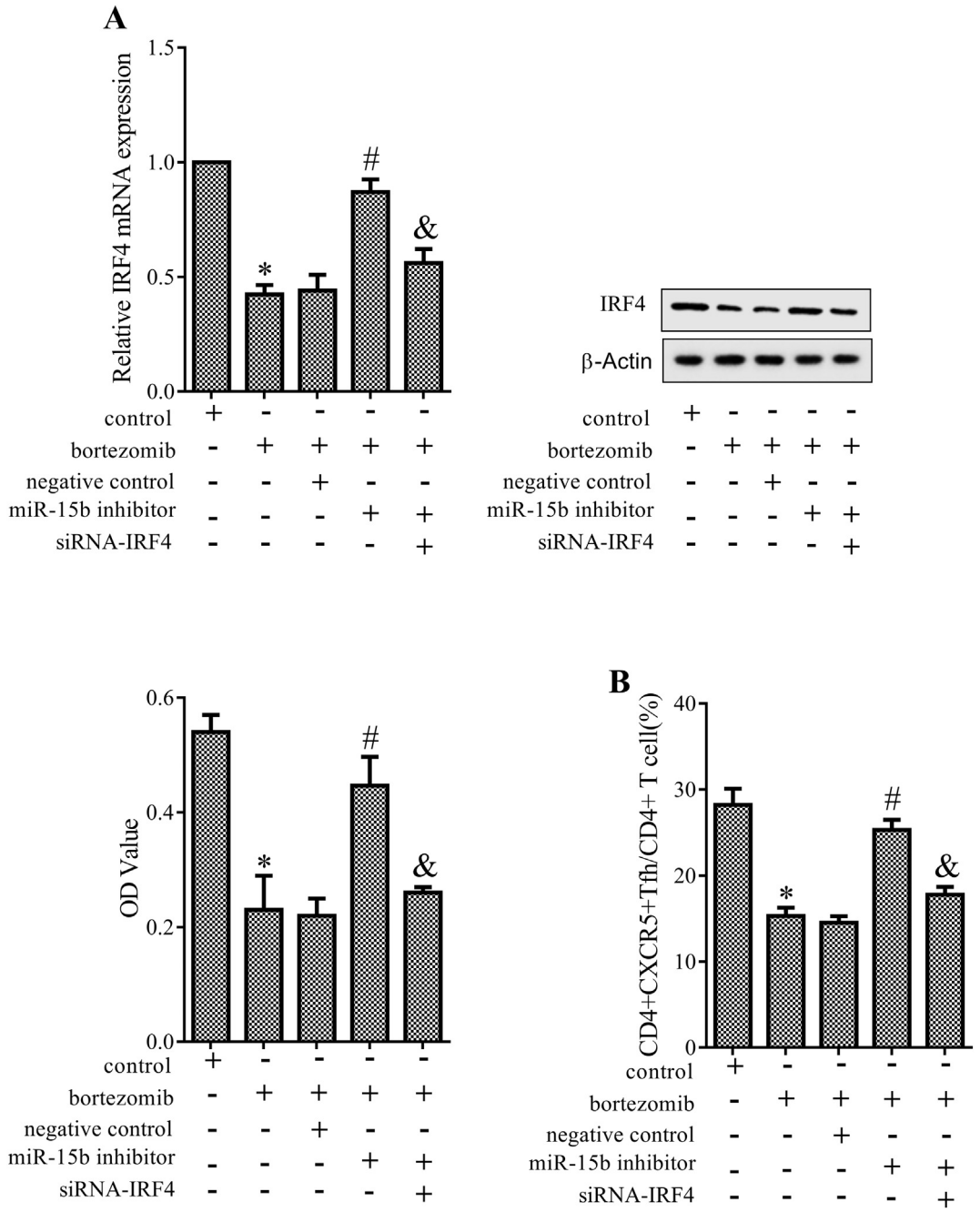

Fig. 6. Bortezomib inhibited Tfh cell proliferation and differentiation through the miR-15b/IRF4 pathway. Tfh cells were divided into 5 groups: control, bortezomib, bortezomib + negative control, bortezomib + miR-15b inhibitor and bortezomib + miR-15b inhibitor + siRNA-IRF4. (A) The expression of IRF4 at mRNA and protein levels in Tfh cells was measured with qRT-PCR and western blotting, and the Tfh cell proliferation was measured by CCK-8 assay; (B) the proportion of Tfh cells ($CD4^+$ $CXCR5^+$) in $CD4^+$ T cells was analyzed using flow cytometry. $^*P < 0.05$ compared with the control group; $^{\#}P < 0.05$ compared with bortezomib + negative control group; $^{\&}P < 0.05$ compared with bortezomib + miR-15b inhibitor group.

luciferase activity in the IRF4-Mut group. To verify our findings, miR-15b mimic or inhibitor were transfected into HEK293T cells followed by evaluation of IRF4 expression at mRNA and protein levels. Our results demonstrated that miR-15b overexpression downregulated IRF4 expression (Fig. 4B, $P < 0.05$), while miR-15b knockdown augmented IRF4 expression (Fig. 4C, $P < 0.05$). Collectively, miR-15b negatively regulated IRF4 expression.

3.5. MiR-15b mediated Tfh cell proliferation and differentiation through regulating IRF4

We further determined whether miR-15b regulated Tfh cell proliferation and differentiation *via* targeting IRF4. The isolated Tfh cells and naïve $CD4^+$ T cells activated by recombinant rat activin A and human IL-12 were respectively randomized into 4 groups: pre-negative control, miR-15b mimic, miR-15b mimic + pcDNA3.1 and miR-15b mimic + pcDNA3.1-IRF4. As a result, a decrease in Tfh cell proliferation (Fig. 5A, $P < 0.05$) and the proportion of Tfh cells ($CD4^+$ $CXCR5^+$) was observed after overexpressing miR-15b (Fig. 5B, $P < 0.05$). Conversely, co-overexpression of miR-15b and IRF4 caused an opposite effect. Conjointly, our finding revealed that miR-15b suppressed the proliferation and differentiation of Tfh cells by directly targeting IRF4.

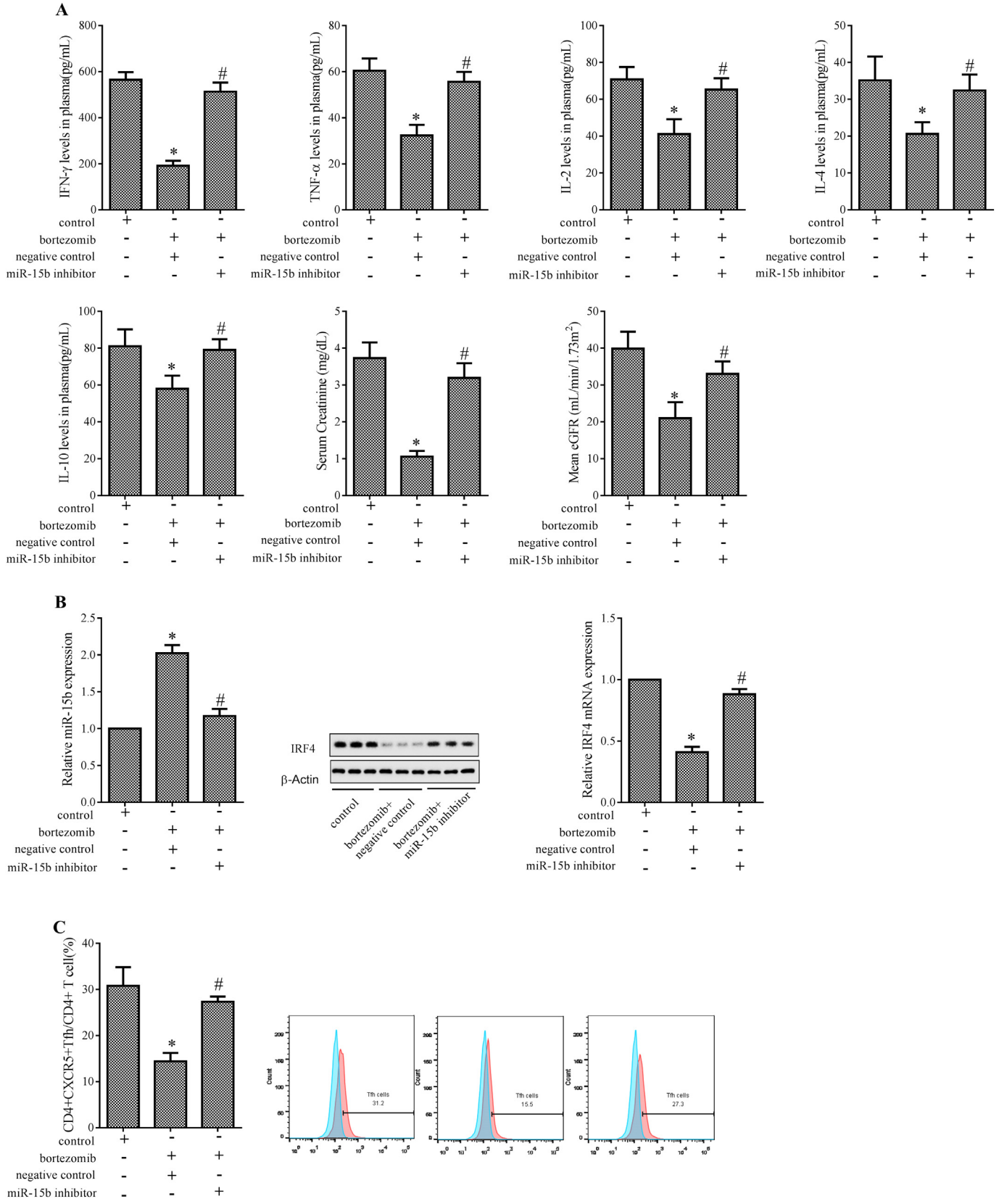

Fig. 7. Bortezomib ameliorated acute rejection in a mouse model of renal allograft *via* upregulating miR-15b. Renal allograft mice were allocated into three groups: control, bortezomib + negative control, and bortezomib + miR-15b inhibitor. (A) The serum levels of IFN-γ, TNF-α, IL-2, IL-4, IL-10 and serum creatinine and mean eGFR of mice were measured; (B) the expression of miR-15b and the expression of IRF4 at mRNA and protein levels were evaluated; (C) the percentage of Tfh cells ($CD4^+$ $CXCR5^+$) in $CD4^+$ T cells was detected. $^*P < 0.05$ compared with control group; $^{\#}P < 0.05$ compared with bortezomib + negative control group.

3.6. Bortezomib-mediated IRF4 downregulation inhibited Tfh cells proliferation and differentiation by upregulating miR-15b

To further investigate the molecular mechanism and biological role of bortezomib affecting Tfh cells proliferation and differentiation, Tfh cells as well as activated naïve $CD4^+$ T cells were randomly divided into 5 groups: control, bortezomib, bortezomib + negative control, bortezomib + miR-15b inhibitor and bortezomib + miR-15b inhibitor + siRNA-IRF4. Cells were treated with 50 nM of bortezomib for 24 h, followed by transfected with miR-15b inhibitor or siRNA-IRF4 for 48 h. It turned out that bortezomib resulted in a larger reduction in IRF4 expression at mRNA and protein levels (Fig. 6A, $P < 0.05$), along with a lower Tfh cells proliferative rate (Fig. 6A, $P < 0.05$) and a decreased percentage of Tfh cells (Fig. 6B, $P < 0.05$) as compared with the control group. On the contrary, an increase in IRF4 expression was observed in cells treated with bortezomib and transfected with miR-15b inhibitor (Fig. 6A, $P < 0.05$), as well the Tfh cells proliferation (Fig. 6A, $P < 0.05$) and the proportion of Tfh cells (Fig. 6B, $P < 0.05$). However, the combination of miR-15b overexpression and IRF4 knockdown restored the function of bortezomib on IRF4 expression and Tfh cells proliferation as well as differentiation, implying that bortezomib effectively inhibited the proliferation and differentiation of Tfh cells through regulation of the miR-15b/IRF4 pathway.

3.7. Bortezomib meliorated acute rejection of renal transplant through decreasing Tfh cells proliferation and differentiation mediated by miR-15b/IRF4 axis in vivo

To validate the functional roles of bortezomib *in vivo*, AR mice were inoculated by bortezomib together with antagomir-15b or negative control, respectively. As expected, the cytokines serum levels, the serum creatinine and mean eGFR (Fig. 7A, $P < 0.05$) in bortezomib group were lower than those in AR group. Moreover, the mRNA expression levels of miR-15b were upregulated, while IRF4 mRNA and protein expression were decreased (Fig. 7B, $P < 0.05$) in addition to the reduction of percentage of Tfh cells (Fig. 7C, $P < 0.05$) after bortezomib injection, nonetheless, bortezomib plus antagomir-15-treatment reversed the trends. Taken together, bortezomib could alleviate acute AR after renal transplant by inhibiting Tfh cells proliferation and differentiation by regulating the miR-15b/IRF4 axis.

4. Discussion

It has been well documented that bortezomib has a critical effect on the treatment of AR after renal transplant [9,10], however little is known about the specific mechanism of bortezomib in the progression of AR. In the present study, we established an AR mouse model to investigate the immunotherapeutic role of bortezomib in renal AR. Our findings displayed that bortezomib regulated IRF4 expression *via* increasing miR-15b, thereby decreasing the proliferation and differentiation of Tfh cells. Lastly, the functional role of bortezomib *in vivo* was clarified, revealing that bortezomib treatment ameliorated renal AR.

In view of the impact of bortezomib on miRNAs expression [20,21], we determined the RNA expression levels of a series of representative miRNAs, including miR-135a, miR-199a-3p, miR-15b, miR-140-3p and miR-130b, in AR group and bortezomib-treated group. Our data demonstrated that bortezomib increased miR-15b expression in AR, suggesting that bortezomib might exert its effect on AR through upregulating miR-15b. Analogously, Jiang et al. [17] have found that bortezomib led to miR-15b upregulation in hepatoma carcinoma cells to promote cell survival. To further explore the biological function of miR-15b in renal AR process, *in vitro* experiments were conducted. We demonstrated that overexpression of miR-15b significantly suppress the proliferation and differentiation of Tfh cells. The current study highlighted the role of miR-15b in AR relief mediated by bortezomib. In regard to how bortezomib can specifically upregulate the 15b miRNA and not the other miRNAs, we hypothetically attribute it to some lncRNAs that could bind with miR-15b [22], which is associated with the role of lncRNAs as competing endogenous RNAs [23]. Such mechanisms deserve further investigations in the future.

In the past years, emerging evidence has considered IRF4 as a pivotal transcription factor in the progression of Tfh cells differentiation [24]. Besides, IRF4 is closely correlated with Treg cell function [25] and it mediates a vital regulatory circuit of T cell dysfunction in transplant [26]. In the B-cell lineage, IRF4 plays an important role in plasma cell differentiation and isotype switching [27]. In this study, we confirmed that IRF4 expression promoted Tfh cell differentiation and demonstrated that IRF4 was a downstream target of miR-15b. In addition, the function of IRF4 in AR after renal transplant was discovered, offering a novel target for AR prevention and treatment.

Although we demonstrated that the serum pro-inflammatory cytokines, such as IFN-γ, TNF-α, IL-2, IL-4 and IL-10, and the serum creatinine, were significantly decreased by bortezomib. The effects of bortezomib on systemic inflammation have not been explored yet, which deserves further interpretation in the future.

In summary, the current study provided a novel insight into the mechanism of AR after renal transplant, demonstrating that bortezomib alleviated AR after renal transplant by regulating miR-15b/IRF4 axis, which contributed to inhibiting Tfh cell proliferation and differentiation. The present study provided significant insight into developing effective measures for prevention and reduction of this negative prognostic factor.

Acknowledgement

Thanks for the supports of the Experimental Animal Center of The First Affiliated Hospital of Zhengzhou University.

References

[1] M. Saatchi, J. Poorolajal, M.A. Amirzargar, H. Mahjub, N. Esmailnasab, Long-term survival rate of kidney graft and associated prognostic factors: a retrospective cohort study, 1994–2011, Ann. Transplant. 18 (2013) 153.
[2] M.I. Ashraf, H.G. Schwelberger, K.A. Brendel, J. Feurle, J. Andrassy, K. Kotsch, H. Regele, J. Pratschke, H.T. Maier, F. Aigner, Exogenous Lipocalin 2 ameliorates acute rejection in a mouse model of renal transplantation, Am. J. Transplant. 16 (2015) 808–820.
[3] C.F. Lee, Y.C. Lo, C.H. Cheng, G. Furtmüller, B. Oh, V. Andrade-Oliveira, A. Thomas, C. Bowman, B. Slusher, M. Wolfgang, Preventing allograft rejection by targeting immune metabolism, Cell Rep. 13 (2015) 760–770.
[4] T.G. Disalvo, J. Narula, A.B. Cosimi, S. Keck, G.W. Dec, M.J. Semigran, Actinomycin D is an effective adjunctive immunosuppressive agent in recurrent cardiac allograft rejection, J. Heart Lung Transplant. 14 (1995) 955.
[5] S. Ge, A. Karasyov, A. Sinha, A. Petrosyan, D. Lovato, D.L. Thomas, A. Vo, S.C. Jordan, M. Toyoda, Cytomegalovirus immunity after alemtuzumab induction in desensitized kidney transplant patients, Transplantation 101 (2017) 1720.
[6] S. Iesari, Q. Lai, E. Favi, F. Pisani, Bortezomib-containing multimodality treatment for antibody-mediated rejection with anti-HLA and anti-AT1R antibodies after kidney transplantation, Yonsei Med. J. 58 (2017) 679–681.
[7] T. Oblak, J. Lindič, J. Gubenšek, R. Kveder, R.A. Aleš, Š. A, H.Ž. Večerić, Š. Borštnar, N. Avguštin, R. Ponikvar, Treatment of antibody-mediated rejection of kidney grafts with bortezomib and/or rituximab compared to standard regimen: experience of Slovene National Center, Clin. Nephrol. 88 (2017).
[8] S. Kizilbash, D. Claes, I. Ashoor, A. Chen, S. Jandeska, R.B. Matar, J. Misurac, J. Sherbotie, K. Twombley, P. Verghese, Bortezomib in the treatment of antibody-mediated rejection in pediatric kidney transplant recipients: a multicenter Midwest Pediatric Nephrology Consortium study, Pediatr. Transplant. 21 (2017) e12873.
[9] J. Waiser, M. Duerr, C. Schönemann, B. Rudolph, K. Wu, F. Halleck, K. Budde, N. Lachmann, Rituximab in combination with Bortezomib, plasmapheresis, and high-dose IVIG to treat antibody-mediated renal allograft rejection, Transplant. Direct 2 (2016) 1.
[10] M.H. Pearl, A.B. Nayak, R.B. Ettenger, D. Puliyanda, M.F. Palma Diaz, Q. Zhang, E.F. Reed, E.W. Tsai, Bortezomib may stabilize pediatric renal transplant recipients with antibody-mediated rejection, Pediatr. Nephrol. 31 (2016) 1341–1348.
[11] V. Staudt, E. Bothur, M. Klein, K. Lingnau, S. Reuter, N. Grebe, B. Gerlitzki, M. Hoffmann, A. Ulges, C. Taube, Interferon-regulatory factor 4 is essential for the developmental program of T helper 9 cells, Immunity 33 (2010) 192–202.
[12] N. Bollig, A. Brüstle, K. Kellner, W. Ackermann, E. Abass, H. Raifer, B. Camara, C. Brendel, G. Giel, E. Bothur, Transcription factor IRF4 determines germinal center formation through follicular T-helper cell differentiation, Proc. Natl. Acad. Sci. U. S.

A. 109 (2012) 8664–8669.
[13] U. Klein, S. Casola, G. Cattoretti, Q. Shen, M. Lia, T. Mo, T. Ludwig, K. Rajewsky, R. Dalla-Favera, Transcription factor IRF4 controls plasma cell differentiation and class-switch recombination, Nat. Immunol. 7 (2006) 773–782.
[14] E.K. van den Akker, F.J. Dor, I.J. JN, R.W. de Bruin, MicroRNAs in kidney transplantation: living up to their expectations? J. Transp. Secur. 2015 (2015) 354826.
[15] M. Matz, C. Lorkowski, K. Fabritius, P. Durek, K. Wu, B. Rudolph, H.H. Neumayer, M.F. Mashreghi, K. Budde, Free microRNA levels in plasma distinguish T-cell mediated rejection from stable graft function after kidney transplantation, Transpl. Immunol. 39 (2016) 52–59.
[16] Y. Singh, O.A. Garden, F. Lang, B.S. Cobb, MicroRNA-15b/16 enhances the induction of regulatory T cells by regulating the expression of Rictor and mTOR, J. Immunol. 195 (2015) 5667–5677.
[17] L. Jiang, D. Zang, S. Yi, X. Li, C. Yang, X. Dong, C. Zhao, X. Lan, X. Chen, S. Liu, A microRNA-mediated decrease in eukaryotic initiation factor 2α promotes cell survival during PS-341 treatment, Sci. Rep. 6 (2016) 21565.
[18] K. Hueper, B. Hensen, M. Gutberlet, R. Chen, D. Hartung, A. Barrmeyer, M. Meier, W. Li, M.S. Jang, M. Mengel, Kidney transplantation: multiparametric functional magnetic resonance imaging for assessment of renal allograft pathophysiology in mice, Investig. Radiol. 51 (2016) 58.
[19] R. Bijkerk, B.W. Florijn, M. Khairoun, J. Duijs, G. Ocak, A.P.J. de Vries, A.F. Schaapherder, M.J.K. Mallat, J.W. de Fijter, T.J. Rabelink, A.J. van Zonneveld, M.E.J. Reinders, Acute rejection after kidney transplantation associates with circulating microRNAs and vascular injury, Transplant. Direct 3 (2017) e174.
[20] Y. Shen, L. Lu, J. Xu, W. Meng, Y. Qing, Y. Liu, B. Zhang, H. Hu, Bortezomib induces apoptosis of endometrial cancer cells through microRNA-17-5p by targeting p21, Cell Biol. Int. 37 (2013) 1114–1121.
[21] Z. Korner, C.C. Fontes-Oliveira, J. Holmberg, V. Carmignac, M. Durbeej, Bortezomib partially improves laminin alpha2 chain-deficient muscular dystrophy, Am. J. Pathol. 184 (2014) 1518–1528.
[22] Y. Chen, Y.J. Lian, Y.Q. Ma, C.J. Wu, Y.K. Zheng, N.C. Xie, LncRNA SNHG1 promotes alpha-synuclein aggregation and toxicity by targeting miR-15b-5p to activate SIAH1 in human neuroblastoma SH-SY5Y cells, Neurotoxicology 68 (2018) 212–221.
[23] Y. Tay, J. Rinn, P.P. Pandolfi, The multilayered complexity of ceRNA crosstalk and competition, Nature 505 (2014) 344–352.
[24] N. Bollig, A. Bruestle, K. Kellner, C. Brendel, M. Huber, R.A. Kroczek, C. Dong, R. Jacob, T.W. Mak, M. Lohoff, A Decisive Role of IRF4 for Tfh Cell Development, European Congress of Immunology, 2012, p. 7.
[25] U. Haljasorg, J. Dooley, M. Laan, K. Kai, R. Bichele, A. Liston, P. Peterson, Irf4 expression in thymic epithelium is critical for thymic regulatory T cell homeostasis, J. Immunol. 198 (2017) 1952–1960.
[26] J. Wu, X. Shi, X. Xiao, L. Minze, J. Wang, R.M. Ghobrial, J. Xia, R. Sciammas, X.C. Li, W. Chen, IRF4 Controls a Core Regulatory Circuit of T Cell Dysfunction in Transplantation, (2017).
[27] A.S. Heimes, K. Madjar, K. Edlund, M.J. Battista, K. Almstedt, S. Gebhard, S. Foersch, J. Rahnenführer, W. Brenner, A. Hasenburg, Prognostic significance of interferon regulating factor 4 (IRF4) in node-negative breast cancer, J. Cancer Res. Clin. Oncol. 143 (2017) 1–9.